

Semi-supervised Semantic Segmentation with Mutual Knowledge Distillation

Jianlong Yuan

Alibaba Group
Beijing, China
gongyuan.yjl@alibaba-inc.com

Zhibin Wang

zhibin.waz@alibaba-inc.com
Hangzhou, China
zhibin.waz@alibaba-inc.com

Jinchao Ge

The University of Adelaide
Adelaide, Australia
jinchao.ge@adelaide.edu.au

Yifan Liu

The University of Adelaide
Adelaide, Australia
yifan.liu04@adelaide.edu.au

ABSTRACT

Consistency regularization has been widely studied in recent semi-supervised semantic segmentation methods, and promising performance has been achieved. In this work, we propose a new consistency regularization framework, termed mutual knowledge distillation (MKD), combined with data and feature augmentation. We introduce two auxiliary mean-teacher models based on consistency regularization. More specifically, we use the pseudo-labels generated by a mean teacher to supervise the student network to achieve a mutual knowledge distillation between the two branches. In addition to using image-level strong and weak augmentation, we also discuss feature augmentation. This involves considering various sources of knowledge to distill the student network. Thus, we can significantly increase the diversity of the training samples. Experiments on public benchmarks show that our framework outperforms previous state-of-the-art (SOTA) methods under various semi-supervised settings. Code is available at [semi-mmseg](#).

CCS CONCEPTS

• **Computing methodologies** → **Scene understanding**.

KEYWORDS

Mutual knowledge distillation, Semi-supervised semantic segmentation, Data and network augmentation, Consistency regularization.

ACM Reference Format:

Jianlong Yuan, Jinchao Ge, Zhibin Wang, and Yifan Liu. 2023. Semi-supervised Semantic Segmentation with Mutual Knowledge Distillation. In *Proceedings of the 31st ACM International Conference on Multimedia (MM '23)*, October 29–November 3, 2023, Ottawa, ON, Canada. ACM, New York, NY, USA, 9 pages. <https://doi.org/10.1145/3581783.3611906>

Permission to make digital or hard copies of all or part of this work for personal or classroom use is granted without fee provided that copies are not made or distributed for profit or commercial advantage and that copies bear this notice and the full citation on the first page. Copyrights for components of this work owned by others than the author(s) must be honored. Abstracting with credit is permitted. To copy otherwise, to publish, to post on servers or to redistribute to lists, requires prior specific permission and/or a fee. Request permissions from permissions@acm.org.

MM '23, October 29–November 3, 2023, Ottawa, ON, Canada.

© 2023 Copyright held by the owner/author(s). Publication rights licensed to ACM.

ACM ISBN 979-8-4007-0108-5/23/10...\$15.00

<https://doi.org/10.1145/3581783.3611906>

1 INTRODUCTION

Segmentation is a fundamental task in visual understanding that aims to classify each pixel in an image into a predefined set of categories. While recent works in semantic segmentation [4, 32, 36, 40, 44, 45] have made significant progress using supervised learning with the use of large-scale datasets [8, 9, 27, 47]. However, labeling such datasets can be labor-intensive and time-consuming for dense prediction problems, requiring up to 60 times more effort than image-level labeling [23]. To address this limitation, semi-supervised learning [2, 29, 41, 42] attempts to learn a model with a limited set of labeled images and a large set of unlabeled images.

State-of-the-art semi-supervised semantic segmentation methods employ consistency regularization to enhance the similarity between the outputs of teacher and student during training. Data augmentations are commonly implemented on images, a practice evidenced by studies such as [39, 41, 42]. Furthermore, they can also be applied to features, as indicated in [28]. Additionally, the utilization of various networks, each possessing distinct initialization parameters, is a common practice, as delineated in [5, 20]. For example, the CPS [5] method feeds the same image into two different initialized networks and uses the pseudo labels generated from one branch to supervise the other branch. However, this method does not preserve important historical information during training. Note that the two branches are optimized with back-propagation without moving average during training. Thus, the model ‘forgets’ important historical information along with the training steps as stated in previous research [13, 15, 31].

To further improve the performance of the semi-supervised semantic segmentation models, we propose a novel mutual knowledge distillation framework. This framework employs two branches of co-training [5] with different initialized parameters and two auxiliary mean teacher models to record the information during the training process and provide extra supervision. The pseudo labels generated from one teacher network supervise the other student and vice versa. Weak augmentation is applied to teacher input images to increase prediction confidence, while input images from the student networks are strongly augmented to diversify samples. Pseudo labels from the teacher network tend to be more reliable, while the student network can be trained on more diverse and challenging samples. We explore feature-level augmentation in student networks, drawing inspiration from the implicit semantic data augmentation technique applied in [33, 34].

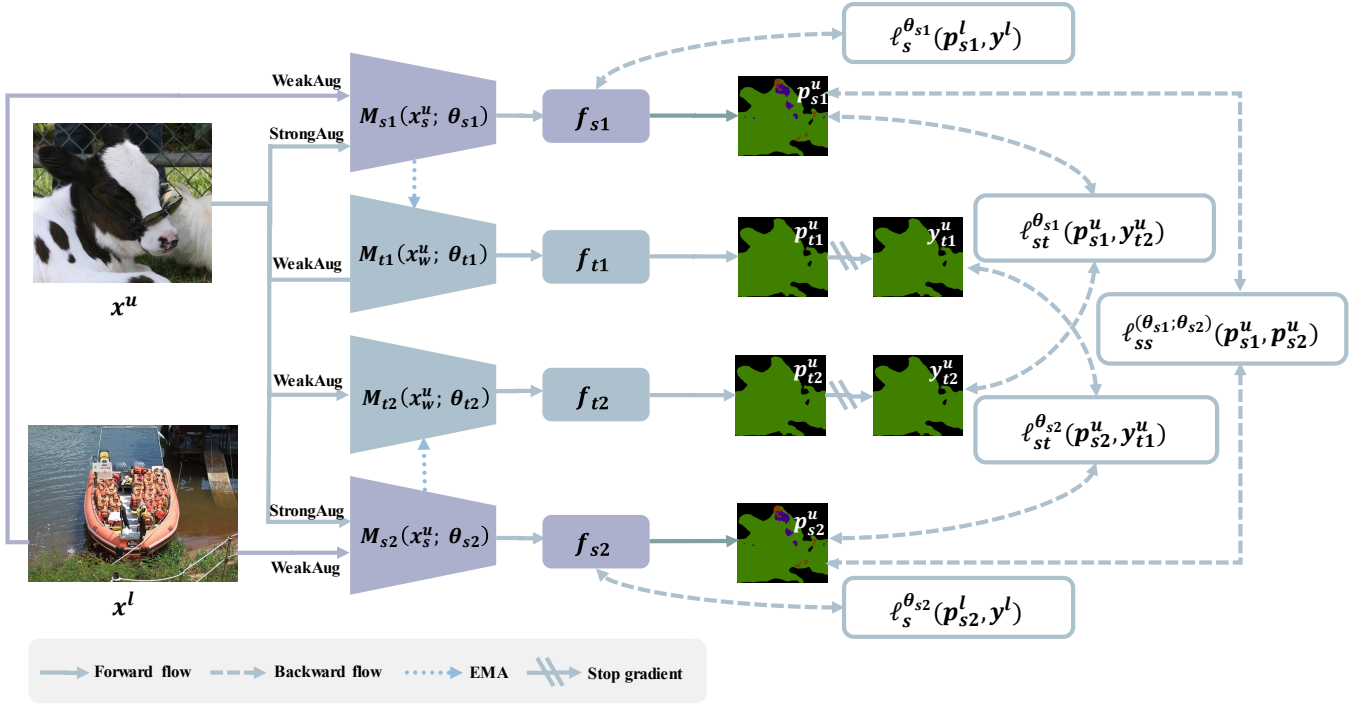


Figure 1: For each image x^u , we apply weak augmentation (WeakAug) on the teacher network and strong augmentation (StrongAug) on the student network. Here p denotes the logits. θ is the parameters of the model and y^u is the one-hot labels generated from p^u . We train the model by minimizing the consistency loss ℓ_{st} and ℓ_{ss} on the unlabeled set and the cross-entropy loss ℓ_s on the labeled set.

Our approach achieves state-of-the-art performance on the PASCAL VOC 2012 [9], Cityscapes [8], and COCO [23] datasets, under various splits of semi-supervised settings. Our main contributions are summarized as follows:

1), We propose the mutual knowledge distillation framework, a new consistency regularization approach for semi-supervised semantic segmentation (S^4). This framework involves two different initialized student networks and two corresponding mean teacher networks. The knowledge from one teacher network is used to supervise the other student branch, and vice versa.

2), We investigate the efficacy of different data augmentation methods for S^4 . Specifically, we discuss feature-level to enhance the diversity of the training dataset. Furthermore, we employ strong and weak augmentations to the student and teacher networks, respectively.

3), We empirically demonstrate the effectiveness of our approach, which achieves state-of-the-art performance on PASCAL VOC 2012, Cityscapes, and COCO datasets under various semi-supervised settings. A detailed ablation study verifies the usefulness of each component in the proposed framework.

2 RELATED WORK

2.1 Semantic segmentation

A variety of methods have been proposed for this task [4, 32, 36, 40, 44, 45], starting with the fully convolutional network (FCN)[25], which trains a pixel-level classifier. It is worth mentioning that our work is based on DeepLabV3Plus [4], which applies a spatial pyramid pooling structure and an encoder-decoder structure to refine object boundaries. The majority of existing approaches in the literature operate under the fully-supervised regime, wherein a significant amount of labeled data is necessary.

2.2 Semi-supervised semantic segmentation

The task of semantic segmentation usually requires a large amount of annotated data, but semi-supervised learning (SSL) offers a new perspective to tackle this problem. SSL methods can be broadly classified into two categories: consistency regularization-based techniques [1, 5, 11, 18, 19, 29–31, 35], and self-training based methods [3, 17, 38, 39, 41, 48].

Consistency-based methods enforce the model to generate the same prediction from augmented images and original ones. Temporal ensembling [22] implements the idea of ensemble multiple checkpoints of students. In particular, mean teacher [1, 31, 32] employs the exponential moving average of the model parameters

to update the weights of the teacher model. Moreover, the student model is supervised under the pseudo-label generated by the teacher model.

Co-training for consistency [5, 20] feeds the same image into two different initialized networks and uses the pseudo labels generated from one branch to supervise the other branch. U²PL[35] designs a method to select reliable annotations from unreliable candidate pixels. Self-training [17, 38, 39, 41] based methods aim at generating pseudo labels to enlarge the training set. They use a teacher model to generate pseudo-labels based on suitable data augmentation and thresholds. Unlike these methods, our approach designs two student networks and two auxiliary mean teacher networks. Furthermore, we apply augmentation to the images and feature augmentation in the same framework, boosting the student network’s performance.

2.3 Data augmentation

We describe data augmentation in SSL from two different perspectives: image-level augmentation [43] and feature-level augmentation [10, 12]. For instance, FixMatch[29] considers weakly-augmented samples as more reliable anchors and constrains its output to be the same as strongly-augmented data. Similarly, UDA [37] uses weakly-augmented data and complex-augmented data to generate similar output. CutMix [42] is a widely adopted technique that generates pseudo labels and implicitly implements the idea of entropy minimization by ensuring the decision boundary passes through a low-density region of the distribution. CCT [28] and GCT [20] use a similar idea to achieve feature augmentation through cross-confidence consistency. Consistency-based SSL methods with auxiliary networks can be considered network-level augmentation. In this paper, we propose applying complex augmentation (image-level augmentation and feature augmentation) to the students and weak augmentation to the teachers.

3 METHOD

We propose a novel consistency regularization framework based on mutual knowledge distillation, as described in Sec. 3.1. The image augmentation method is discussed in Sec. 3.2. Finally, the training procedure is introduced in Sec. 3.3. We aim at training an end-to-end segmentation model with a massive amount of unlabeled and few labeled data in a semi-supervised learning manner.

3.1 Mutual Knowledge Distillation Framework

Overview. We first present the settings for a typical semi-supervised semantic segmentation task. Labeled datasets and unlabeled datasets are denoted as $D^l = \{(\mathbf{x}_i^l, \mathbf{y}_i^l)\}_{i=1}^{|D^l|}$ and $D^u = \{(\mathbf{x}_i^u)\}_{i=1}^{|D^u|}$ with $|D^l| \ll |D^u|$, where $\mathbf{x}_i \in \mathbb{R}^{H \times W \times 3}$ is the input RGB image with the size of $H \times W$ and $\mathbf{y}_i \in \mathbb{R}^{H \times W \times C}$ represents the pixel-level one-hot label map for C classes. The proposed MKD framework is illustrated in Figure 1, which consists of four branches: two baseline student networks and two auxiliary mean teacher networks. The labeled images are fed into the student network and optimized with the normal cross-entropy loss \mathcal{L}_s between ground truth labels. The unlabeled images with strong (weak) augmentation are fed into the student (teacher) networks. Each student network is trained under the supervision of the pseudo labels generated by the other student

network (\mathcal{L}_{ss}) and by the other teacher network (\mathcal{L}_{st}). The knowledge between the two branches is transferred with the proposed MKD framework. Details for each part are described as follows.

Baseline student networks. The co-training methodology entails the establishment of two networks, each exhibiting identical structures but divergent initializations. This process is further characterized by the imposition of constraints to ensure consistency between the outputs of the two networks. Our baseline student networks are based on the previous state-of-the-art co-training method, CPS [5]. Student networks are defined as M_{s1} and M_{s2} , respectively. Network structures for M_{s1} and M_{s2} are the same, but the parameters are initialized differently with θ_{s1} and θ_{s2} . For example, given an input image \mathbf{x} , the baseline student networks produce features denoted as f_{s1} and f_{s2} , respectively. Following the typical co-training baseline [5], each student network is supervised by the pseudo labels generated by the other student network, which is denoted as \mathcal{L}_{ss} .

Auxiliary mean teacher networks. Prior research, as demonstrated in [13, 15, 31], has illustrated the potential of mean teacher models to store and leverage historical information, thereby enhancing model performance. It does not need to be optimized, thus adding relatively little computation. Building on this idea, we incorporate two auxiliary mean teacher networks denoted as M_{t1} and M_{t2} into our MKD framework. The network structure of the teacher is the same as the network structure of the student. However, the mean teacher does not require back-propagation during training. The corresponding student model updates the mean teacher parameters according to exponential moving average(EMA) as Eq. (1), where γ controls the speed of updates and $i \in [1, 2]$ represents the index of the branch being updated:

$$\theta_{ti} = \gamma\theta_{ti} + (1 - \gamma)\theta_{si}. \quad (1)$$

Mutual knowledge distillation. As illustrated in Figure 1, labeled samples are used to train student models, and losses are calculated using supervised loss. Unlabeled samples, after strong augmentation, are fed into the two student models to obtain different outputs (p_{s1}^u, p_{s2}^u). Similarly, to generate more reliable supervision, samples after weak augmentation are fed into the two teacher models to obtain different outputs (p_{t1}^u, p_{t2}^u). There are two main objectives for the proposed MKD framework. First, we enable the teacher network to update smoothly and produce high-confidence predictions on easy samples. Second, we allow the student network to learn from more challenging samples and get more useful information. Thus, we apply all levels of augmentation to the samples fed into the student network. By adding two auxiliary mean teacher networks, we can obtain reliable supervision, which is not easy to collapse. To apply the network augmentation, the output pseudo label \mathbf{y}_{t1}^u from the M_{t1} is used to supervise the logits map \mathbf{p}_{s2}^u from M_{s2} , and vice versa. Eq. (2) is the consistency loss between teacher and student models:

$$\mathcal{L}_{st}^u = \ell_{st}^{\theta_1}(\mathbf{p}_{s1}^u, \mathbf{y}_{t2}^u) + \ell_{st}^{\theta_2}(\mathbf{p}_{s2}^u, \mathbf{y}_{t1}^u). \quad (2)$$

where \mathbf{y}_{t1}^u and \mathbf{y}_{t2}^u denotes one hot labels of the teachers’ outputs. **Knowledge selection.** We add a threshold on the teacher branch to confirm the training process supervised under higher confidence.

This process is called knowledge selection, where the threshold ensures that the teacher is confident about transferring knowledge to students during the distillation process. By selecting a threshold greater than 0.95, we leave noisy signals out and keep the supervision between student and teacher reliable. And we found that if the threshold is applied to the supervision between the student and the other student, some useful information is lost in this process, and worse results will be obtained. Following Eq. (3), we add a threshold to achieve the knowledge selection. T is set to be 0.95 by default in Eq. (3):

$$\mathcal{L}_{st}^u = \ell_{st}^{\theta_1}(\mathbf{p}_{s1}^u, \mathbf{y}_{t2}^u | (\mathbf{p}_{s2}^u \geq T)) + \ell_{st}^{\theta_2}(\mathbf{p}_{s2}^u, \mathbf{y}_{t1}^u | (\mathbf{p}_{s1}^u \geq T)). \quad (3)$$

3.2 Augmentation

Pseudo-labels are generated by the model itself and provide limited information. To increase the diversity of the samples for the student network in our MKD framework, we apply image-level augmentations.

Image augmentation. Image augmentation is based on weak and strong augmentation pairs. Weak data augmentation (WDA) (e.g. image flipping, cropping, resizing) is applied to the images passed to the teacher models. In addition, strong data augmentation (SDA) (e.g. image flipping, cropping, resizing, cutMix, random select an operator from color jitter, blur, gray-scale, equalize and solarize) is applied to the same ones fed to the student model to improve overall generalization. Motivated by the distribution of batch normalization [41], we do not consider many strong color augmentation operations. Particularly, the CutMix [42] augmentation is achieved by applying a binary mask m that combines two images using the function $x = (1 - m) \odot x_i + m \odot x_j$. We apply CutMix by combining two input images in the batch for student models and use the same binary mask on the feature of teachers' logits with $p = (1 - m) \odot p_i + m \odot p_j$. Then we apply p to supervising students. **Feature augmentation.** Feature Data Augmentation (FDA) employs limitless meaningful semantic transformations to modify the feature spaces. This method tweaks the image semantically without the need for an auxiliary network. FDA works by finding suitable translation vectors in the feature space and generating an enhanced feature set. For this enhancement process, category information is essential. However, for unlabeled data where such information is absent, we use pseudo-labels as a replacement.

When applying FDA to semi-supervised semantic segmentation, we meticulously augment each feature to develop an improved feature set. The network's refinement is achieved by reducing the cross-entropy (CE) loss. If we consider M tending towards infinity, we can compute the CE loss for all feasible augmented features. The upper bound of this loss is presented in Eq. (4).

$$\mathcal{L}_{\infty}(\theta | \Sigma) \leq \frac{1}{N} \sum_{i=1}^N \log \left(\sum_{j=1}^C e^{\mathbf{v}_{j y_i}^T \mathbf{f}_i + (b_j - b_{y_i}) + \frac{\lambda}{2} \mathbf{v}_{j y_i}^T \Sigma y_i \mathbf{v}_{j y_i}} \right). \quad (4)$$

To incorporate semantic augmentation for semi-supervised semantic segmentation, we analyze the structure of the ISDA loss. Eq. (4) ends up with just one more term than the standard cross-entropy loss. Thus, each pixel in the student's features can be calculated by $\mathbf{p}_s = \mathbf{v}^T \mathbf{f}_s + b + \frac{\lambda}{2} \mathbf{v}^T \Sigma \mathbf{v}$. Pseudo-labels are used to obtain the

category information required for feature augmentation. Further details can be found in the supplementary materials.

3.3 Optimization of the Framework

The full training loss for the whole framework is described in Eq. (5), where α and β are the loss weights.

$$\mathcal{L} = \mathcal{L}_s^l + \alpha \mathcal{L}_{st}^u + \beta \mathcal{L}_{ss}^u, \quad (5)$$

The first loss in Eq. (5) is the supervised segmentation loss for student models, defined as Eq. (6), where ℓ_{ce} is the cross-entropy loss function, \mathbf{y} presents the ground truth, and θ_1 and θ_2 are model parameters of different students.

$$\mathcal{L}_s^l = \ell_{ce}^{\theta_1}(\mathbf{p}_{s1}^l, \mathbf{y}^l) + \ell_{ce}^{\theta_2}(\mathbf{p}_{s2}^l, \mathbf{y}^l), \quad (6)$$

The second term is described in Eq. (2), which is the consistency loss based on cross-entropy. The last term \mathcal{L}_{ss}^u in Eq. (5) is the consistency loss between students same as CPS [5].

$$\mathcal{L}_{ss}^u = \ell_{ss}^{\theta_1}(\mathbf{p}_{s1}^u, \mathbf{y}_{s2}^u) + \ell_{ss}^{\theta_2}(\mathbf{p}_{s2}^u, \mathbf{y}_{s1}^u). \quad (7)$$

We show our MKD framework in Algorithm 1. First, we initialize student models with different random initialization parameters and set the same parameters for its teacher network. Then, after obtaining augmented data from the input images with SDA and WDA, we first use EMA to update the teachers' parameters. Finally, as described in Fig. 1, we follow Eq. (5) to train the model.

Algorithm 1: Mutual Knowledge Distillation

- 1 Initialize $\mathcal{L} \leftarrow 0$.
 - 2 Sample labeled images x^l and corresponding labels y^l from D^l .
 - 3 Sample unlabeled images without labels x^u from D^u .
 - 4 **Initialization Student** Randomly initialize two student models.
 - 5 **Initialization Teacher** Apply the same initialization of each student to the corresponding teacher.
 - 6 **for** step = 1, ..., n **do**
 - 7 Update momentum of M_{t1}, M_{t2} .
 - 8 Apply weak data augmentation on x_w^l, x_w^u .
 - 9 Obtain strongly augmented x_s^u as described in Sec. 3.2.
 - 10 Generate p_{t1}^u, p_{t2}^u as unlabeled probabilities.
 - 11 Gain labeled probabilities: p_{s1}^l, p_{s2}^l .
 - 12 Get featured augmented p_{s1}^u, p_{s2}^u based on Eq. (3.2).
 - 13 Calculate the whole loss as described in Eq. (2), (5), (6), (7).
 - 14 **end**
-

4 EXPERIMENTS

4.1 Implementation Details

Datasets. Following previous methods [5, 35, 41], experiments are performed on three widely used image segmentation datasets, PASCAL VOC 2012 (VOC) [9], Cityscapes [8] and COCO [23]. VOC [9] is a standard semantic segmentation benchmark with 21 classes, including the background. The standard VOC datasets have 1464 images for training, 1449 images for validation, and 1456 images for testing. Following the previous works [4], we combine VOC with 9118 training images from the Segmentation Boundary Dataset (SBD) [14] as VOCAug. During training on VOCAug and VOC, we employ a crop size of 512×512 .

Cityscapes [8] consists of 2975/500/1525 finely annotated urban scene images with resolution 2048×1024 for train/validation/test,

Table 1: Compared with state-of-the-art methods on the Pascal VOC 2012 val set under different partition protocols. Here ‘1/n’ means that we use ‘1/n’ labeled dataset and the remaining images in the training set are used as the unlabeled dataset. † means we introduce the unlabeled dataset with a total of 10582 images. * denotes an enhanced training scheme, which will be further discussed in Table 4. SupOnly stands for supervised training without using any unlabeled data. Blue text indicates the performance between our methods compared with the supervised-only method.

Method	1/16 (92)	1/8 (183)	1/4 (366)	1/2 (732)	Full (1464)
SupOnly-R50	43.97	49.57	57.76	65.73	68.81
SupOnly-R101	45.77	54.92	65.88	71.69	72.50
CCT-R50 [28]	33.10	47.60	58.80	62.10	69.40
MT-R101 [31]	48.70	55.81	63.01	69.16	-
AdvSemSeg-R101 [19]	39.69	47.58	59.97	65.27	68.40
VAT-R101 [26]	36.92	49.35	56.88	63.34	-
CutMix-Seg-R101 [42]	55.58	63.20	68.36	69.84	-
PC ² Seg-R101 [46]	57.00	66.28	69.78	73.05	74.15
GCT-R101 [20]	46.04	54.98	64.71	70.67	-
PseudoSeg-R101 [48]	57.60	65.50	69.14	72.41	73.23
CPS-R101 [5]	64.07	67.42	71.71	75.88	-
SimpleBaseline-R101 [41]	-	-	-	-	75.00
Ours-R50	60.60	66.74	71.01	72.73	78.14
Ours-R101	65.35 (+19.58)	70.18 (+15.26)	74.44 (+8.56)	75.90 (+4.21)	79.96 (+7.46)
PS-MT-R101 [24] [†]	65.80	69.58	76.57	78.42	80.01
ST+-R101 [39] [†]	65.20	71.00	74.60	77.30	79.10
U ² PL-R101 [35] [†]	67.98	69.15	73.66	76.16	79.49
Ours-R101 [†]	69.10	74.63	76.76	78.66	80.02
Ours-R101 [†] *	76.12 (+30.35)	77.83 (+22.91)	80.40 (+14.52)	82.13 (+10.44)	83.78 (+11.28)

respectively. The segmentation performance is evaluated over 19 challenging categories. We use a training crop size of 1024×512 .

We have chosen the COCO dataset [23] for our experiments to conduct further benchmarking of the proposed method. It is a challenging benchmark for semantic segmentation composed of 118k/5k for training/validation. We employ a crop size of 512×512 . **Training.** Our method is implemented on MMSegmentation [7]. Following DeepLabV3Plus [4], we use the ‘‘poly’’ learning rate policy where the initial learning rate is multiplied by $(1 - \text{iter}/\text{iter}_{\max})^{0.9}$. For VOC and COCO datasets, the initial learning rate is set to 0.0025, while for Cityscapes, it is set to 0.01. Specifically, the batch size is set to 16 for all datasets, and all training was performed on the four NVIDIA A100. We train the network with mini-batch stochastic gradient descent (SGD). The momentum is fixed as 0.9, and the weight decay is set to 0.0005.

Network architecture. We use DeepLabv3plus [4] with ResNet [16] pre-trained on ImageNet [21] as our segmentation network for VOC and Cityscapes datasets. The decoder head is composed of separable convolution same as standard DeepLabv3plus. It is worth noting that we do not use any tricks in the model structure. We adopt Xception-65 [6] as our backbone network for the COCO datasets, following the same architectural design as other methods for a fair comparison.

Evaluation metrics. Following [4], we adopt the mean Intersection over Union (mIoU) as the evaluation metrics. All results are

estimated on the validation set. Particularly, we report results via only single-scale testing.

4.2 Comparison with State-of-the-art Methods

We conduct the comparison experiments with state-of-the-art algorithms in Table 1, Table 2, and Table 3.

Results on PASCAL VOC 2012 dataset. Table 1 shows comparison results on PASCAL VOC 2012 dataset. Following previous settings, we sample labeled images from 1) the original VOC 1464 training images, and 2) VOCAug with a total of 10582 images. It is important to notice that the methods with † and without † only differ in unlabeled images. They share the same ‘1/n’ labeled data set and validation set with 1449 images. On the first data splits, assuming 1464 images in total for training, the proposed framework accomplishes 1.28%, 2.76%, 2.73%, with only 92, 183, and 366 labeled images under ResNet-R101 compared with CPS-R101 [5].

Note that we achieve similar performance with CPS [5] under 1/16 partitions, which is trained with only 92 label images as the number of labeled images is too small to generate reliable labels for the teacher network. As shown in Table 1, our method improved by 30.35% based on ResNet-101 compared with the supervised-only method with only 92 labeled images on VOCAug. When additional unlabeled data are incorporated, we adopt the identical splits used in previous works such as [24, 35, 39].

Table 2: Comparison with state-of-the-art on the PASCAL VOCAug and Cityscapes val set under different partition protocols. The VOCAug trainset consists of 10,582 labeled samples in total. ‡ means the same split as U²PL. Other methods use the same split as CPS. ★ presents the approach reproduced by [35]. (-) means data is not available. The underline represents the best result of the CPS split. The best results of the U²PL split are shown in bold. SupOnly stands for supervised training without using any unlabeled data. Blue text indicates the performance between our methods compared with the supervised-only method.

Method	ResNet-50				ResNet-101			
	1/16(662)	1/8(1323)	1/4(2646)	1/2(5291)	1/16(662)	1/8(1323)	1/4(2646)	1/2(5291)
<i>Pascal VOC 2012</i>								
SupOnly	62.40	68.20	72.30	-	70.60	73.12	76.35	77.21
SupOnly [‡]	-	-	-	-	67.87	71.55	75.80	77.13
MT [31]	66.77	70.78	73.22	75.41	70.59	73.20	76.62	77.61
CCT [28]	65.22	70.87	73.43	74.75	67.94	73.00	76.17	77.56
CutMix-Seg [42]	68.90	70.70	72.46	74.49	72.56	72.69	74.25	75.89
GCT [20]	64.05	70.47	73.45	75.20	69.77	73.30	75.25	77.14
CPS [5]	68.21	73.20	74.24	75.91	72.18	75.83	77.55	78.64
CPS w/ CutMix [5]	71.98	73.67	74.90	76.15	74.48	76.44	77.68	78.64
PS-MT [24]	72.83	75.70	76.43	77.88	75.50	78.20	78.72	79.76
ST++ [39]	73.20	75.50	76.00	-	74.70	77.90	77.90	-
U ² PL [‡] [35]	-	-	-	-	77.21	79.01	79.30	80.50
Ours	<u>76.88</u> (+14.48)	<u>78.25</u> (+10.05)	<u>79.23</u> (+6.93)	<u>79.74</u> (-)	<u>78.65</u> (+8.05)	<u>80.11</u> (+6.99)	<u>80.75</u> (+4.40)	<u>81.72</u> (+4.51)
Ours [‡]	<u>77.99</u> (-)	<u>78.49</u> (-)	<u>78.86</u> (-)	<u>78.19</u> (-)	<u>80.05</u> (+12.18)	<u>81.35</u> (+9.80)	<u>82.30</u> (+6.50)	<u>80.60</u> (+3.47)
<i>Cityscapes</i>								
ResNet-50								
ResNet-101								
1/16(186) 1/8(372) 1/4(744) 1/2(1488) 1/16(186) 1/8(372) 1/4(744) 1/2(1488)								
SupOnly	-	70.80	73.70	-	62.96	69.81	74.23	77.46
SupOnly [‡]	-	-	-	-	65.74	72.53	74.43	77.83
MT [31]	66.14	72.03	74.47	77.43	68.08	73.71	76.53	78.59
CCT [28]	66.35	72.46	75.68	76.78	69.64	74.48	76.35	78.29
CutMix-Seg [11]	-	-	-	-	72.13	75.83	77.24	78.95
GCT [20]	65.81	71.33	75.30	77.09	66.90	72.96	76.45	78.58
CPS [5]	69.79	74.39	76.85	78.64	70.50	75.71	77.41	80.08
CPS w/ CutMix [5]	<u>74.47</u>	76.61	77.83	78.77	74.72	<u>77.62</u>	<u>79.21</u>	80.21
CPS [‡] ★ [5]	-	-	-	-	69.78	74.31	74.58	76.81
SimpleBaseline [41]	-	-	-	-	-	74.10	77.80	78.70
PS-MT [24]	-	<u>77.12</u>	78.38	79.22	-	-	-	-
U ² PL [‡] [35]	-	-	-	-	70.30	74.37	76.47	79.05
Ours	<u>75.47</u> (-)	<u>78.07</u> (+7.27)	<u>79.95</u> (+6.25)	<u>80.52</u> (-)	<u>77.19</u> (+14.23)	<u>79.20</u> (+9.39)	<u>80.80</u> (+6.57)	<u>81.04</u> (+3.58)
Ours [‡]	73.14 (-)	75.00 (-)	<u>78.62</u> (-)	<u>79.90</u> (-)	<u>75.31</u> (+9.57)	75.98 (+3.45)	78.28 (+3.85)	<u>80.74</u> (+2.91)

Table 3: Comparison with state-of-the-art on the COCO [23] dataset based on Xception-65 [6] under different partition protocols. SupOnly stands for supervised training without using any unlabeled data. Blue text indicates the performance between our methods compared with the supervised-only method.

Method	1/512(232)	1/256(463)	1/128(925)	1/64(1849)	1/32(3697)
SupOnly	22.9	28.0	33.6	37.8	42.2
PseudoSeg [48]	29.8	37.1	39.1	41.8	43.6
PC ² Seg [46]	29.9	37.5	40.1	43.7	46.1
Ours	<u>36.7</u> (+13.8)	<u>43.7</u> (+15.7)	<u>48.9</u> (+15.3)	<u>51.0</u> (+13.2)	<u>54.1</u> (+11.9)

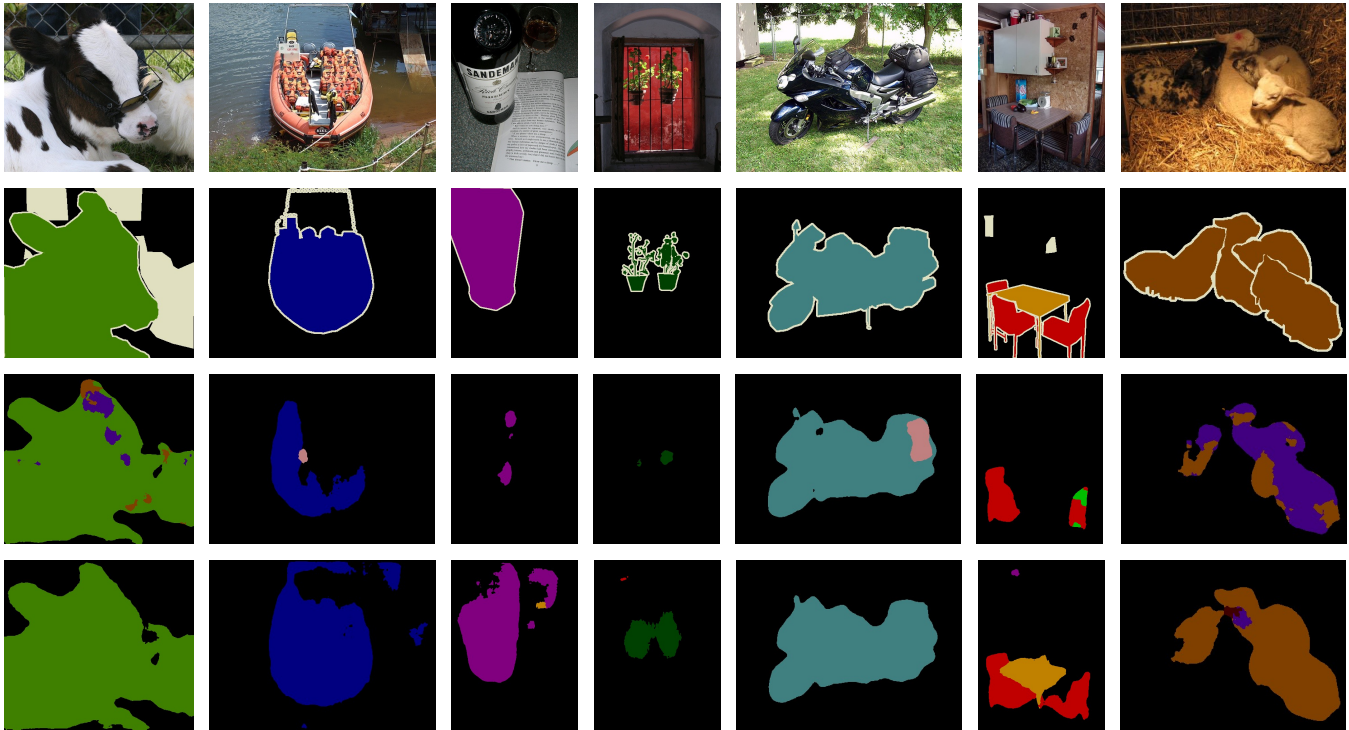


Figure 2: Qualitative results on the PASCAL VOC 2012 datasets using 1/16 (662) labeled samples and ResNet50. The first line exhibits the input images. The second line shows the ground truth. The third line presents the baseline of co-training. The fourth line displays our method.

Our method still gains remarkable performance based on ResNet-101. It shows that more unlabeled images could bootstrap performance. In particular, compared with the U²PL method, our method improves by 8.14% and 8.38% under 1/16 and 1/8 partition protocols. It is also demonstrated that our method is more effective on fewer data. In addition, we set a confidence of 0.95 for selecting regions with higher confidence to select useful knowledge. The results are reported at the last line in table 1.

Table 2 compares our method with the other state-of-the-art methods on VOCAug. To make a fair comparison, we train our MKD framework under two different split lists following previous work. Using the same split as CPS, the proposed method performs favorably against the previous state-of-the-art methods. Furthermore, as the amount of data increases, the performance gap between the various methods becomes smaller, proving that the segmentation task does not require a lot of labeled data.

Figure 2 shows the quantitative results of different methods on the PASCAL VOC 2012 datasets. We can see that co-training can not reasonably separate the objects (especially large-sized objects such as cows, boats, sheep, and motorbikes) completely while ours corrects these errors. Compared to co-training, our method performs well on these complex examples, such as potted plant and chair.

Results on Cityscapes dataset. The Cityscapes dataset consists of images focusing on urban scenes. As shown in Table 2, our method achieves notable improvements under various partition protocols

with the same split as CPS [5]. In addition, we improve by 5.01% under 1/16(186) partition protocol with the same split as U²PL [35]. Our method outperforms the existing state-of-the-art method by a notable margin. Specifically, we report results with single-scale testing. We attribute this significant improvement to the fact that the Cityscapes dataset is relatively redundant so the teacher model can provide more accurate pseudo-labeling.

Results on the COCO dataset. The COCO dataset is a quite challenging task with 118k training images, consisting of 81 classes in total. As shown in Table 3, our method achieves much better results compared with PC²Seg [46] based Xception-65 [6] under 1/512, 1/256, 1/128, 1/64 and 1/32 partition protocols the same as PseudoSeg [48]. In addition, we improve by 6.2%-8.8% with the same split as PC²Seg [46]. Our method outperforms the existing state-of-the-art method by a notable margin.

4.3 Ablation Study

In this subsection, we conduct experiments to explore the effectiveness of each proposed module on the VOC dataset under different semi-supervised settings.

Effectiveness of mutual knowledge distillation. As illustrated in Table 4, we conduct a series of experiments to identify each module’s performance. We take co-training as our baseline, the same as CPS [5]. We first try to add naive mean teacher (MT) and find that the results do not improve or reduce and even lead to training instability. It may be because the teacher and student models are too similar, leading to collapse. By adding the mutual

Table 4: Ablation study on the proposed semi-supervised learning framework. The model here is Deeplabv3Plus with ResNet101 backbone. Co-training denotes the baseline the same as CPS. Mutual MT presents mutual knowledge distillation. SDA denotes strong data augmentation. KS is knowledge selection. FDA denotes feature data augmentation

Co-training	Mutual MT	SDA	KS	FDA	1/16(662)	1/8(1323)	1/4(2646)	1/2(5291)
✓					72.18	75.83	77.55	78.64
✓	✓				75.19	77.92	79.76	81.03
✓	✓			✓	77.52	78.53	79.45	80.63
✓		✓			74.48	76.44	77.68	78.64
✓	✓	✓			78.00	79.49	80.66	80.77
✓	✓	✓	✓		78.65	80.11	80.75	81.72

Table 5: Ablation study of the knowledge selection with different components \mathcal{L}_{ss} and \mathcal{L}_{st} . It uses R101 as the backbone with PseudoSeg splits.

\mathcal{L}_{st}	\mathcal{L}_{ss}	1/16(92)	1/8(183)	1/4(366)	1/2(732)	Full(1464)
✓		74.72	77.16	79.15	80.45	81.81
	✓	73.20	75.65	78.42	80.23	82.39
✓	✓	73.41	75.64	78.71	80.30	82.12

Table 6: Ablation study of the heterogeneous network augmentation, which uses ResNet101 as the backbone. SN means the same network, and HN means heterogeneous network.

HN	SN	1/16(92)	1/8(183)	1/4(366)	1/2(732)	Full(1464)
✓		74.89	77.63	79.48	81.13	82.54
	✓	76.12	77.83	80.40	82.13	83.78

mean teacher, the collapse disappeared, which resulted in a 3.01% performance improvement under 1/16 (662).

Effectiveness of data augmentation. In Table 4, to introduce more augmentation, we also added the strategies of strong augmentation(SDA) which accompanied 2.30% performance improvement under 1/16(662) partition protocols. Combining SDA and Mutual MT, we improve original co-training from 72.18% to 78.00% resulting in a 5.82% gain. The final combination of all methods obtains the best result and yields a performance improvement of 6.47% under 1/16(662) partition protocols.

Ablation study on feature augmentation. We conducted an ablation study on the effect of feature augmentation using the ResNet101 backbone on the CPS splits. Our results indicate that the proposed approach yields a performance boost of 2.33% and 0.61% for 1/16 and 1/8 labeled data ratios, respectively. However, we also observed that this approach can harm training performance when the labeled data is overwhelming. The details of this are discussed in the supplementary section.

Ablation study on knowledge selection. The Table 5 shows the effectiveness of the knowledge selection with different components \mathcal{L}_{ss} and \mathcal{L}_{st} . It can be seen that the knowledge selection applied on \mathcal{L}_{st} is superior to others, indicating that the improvement brought by knowledge selection applied to students and teachers will leave noise out with lower confidence. And the simple form of knowledge

selection with a 0.95 threshold is reliable, but other reasonable values are also acceptable.

Ablation study on heterogeneous network augmentation. To assess the effectiveness of our method, we conducted an experiment comparing the same model architecture with the heterogeneous network (HN) models, which employed PSPNet and Deeplabv3plus as teachers. The results, shown in Table 6, indicate that our method achieved a 1.23% improvement over the HN under the 1/16 (662) partition protocol, demonstrating the superiority of our method.

5 CONCLUSION

We have proposed a new consistency learning scheme, called mutual knowledge distillation, for semantic segmentation. Our method utilizes two auxiliary mean-teacher models and a combination of strong-weak augmentation and feature augmentation to increase the diversity of training samples for the student network. Experimental results show that our proposed method outperforms recent state-of-the-art methods on several benchmark datasets for semantic segmentation, including PASCAL VOC 2012, Cityscapes, and Microsoft COCO. Notably, our framework achieves significant performance improvements even when labeled data is limited.

REFERENCES

- [1] David Berthelot, Nicholas Carlini, Ekin D Cubuk, Alex Kurakin, Kihyuk Sohn, Han Zhang, and Colin Raffel. 2019. Remixmatch: Semi-supervised learning with distribution alignment and augmentation anchoring. *Proc. IEEE Conf. Comp. Vis. Patt. Recogn.* (2019).
- [2] David Berthelot, Nicholas Carlini, Ian Goodfellow, Nicolas Papernot, Avital Oliver, and Colin A Raffel. 2019. Mixmatch: A holistic approach to semi-supervised learning. *Proc. Advances in Neural Inf. Process. Syst.* 32 (2019).
- [3] Liang-Chieh Chen, Raphael Gontijo Lopes, Bowen Cheng, Maxwell D Collins, Ekin D Cubuk, Barret Zoph, Hartwig Adam, and Jonathon Shlens. 2020. Naive-student: Leveraging semi-supervised learning in video sequences for urban scene segmentation. In *Proc. Eur. Conf. Comp. Vis.* Springer, 695–714.
- [4] Liang-Chieh Chen, Yukun Zhu, George Papandreou, Florian Schroff, and Hartwig Adam. 2018. Encoder-decoder with atrous separable convolution for semantic image segmentation. In *Proc. Eur. Conf. Comp. Vis.* 801–818.
- [5] Xiaokang Chen, Yuhui Yuan, Gang Zeng, and Jingdong Wang. 2021. Semi-Supervised Semantic Segmentation with Cross Pseudo Supervision. In *Proc. IEEE Conf. Comp. Vis. Patt. Recogn.* 2613–2622.
- [6] François Chollet. 2017. Xception: Deep learning with depthwise separable convolutions. In *Proc. IEEE Conf. Comp. Vis. Patt. Recogn.* 1251–1258.
- [7] MMSegmentation Contributors. 2020. MMSegmentation: OpenMMLab Semantic Segmentation Toolbox and Benchmark. <https://github.com/open-mmlab/mms Segmentation>.
- [8] Marius Cordts, Mohamed Omran, Sebastian Ramos, Timo Rehfeld, Markus Enzweiler, Rodrigo Benenson, Uwe Franke, Stefan Roth, and Bernt Schiele. 2016. The cityscapes dataset for semantic urban scene understanding. In *Proc. IEEE Conf. Comp. Vis. Patt. Recogn.* 3213–3223.
- [9] Mark Everingham, SM Eslami, Luc Van Gool, Christopher KI Williams, John Winn, and Andrew Zisserman. 2015. The pascal visual object classes challenge: A retrospective. *Int. J. Comput. Vision* 111, 1 (2015), 98–136.
- [10] Zhengyang Feng, Qianyu Zhou, Qiqi Gu, Xin Tan, Guangliang Cheng, Xuequan Lu, Jianping Shi, and Lizhuang Ma. 2022. Dmt: Dynamic mutual training for semi-supervised learning. *Pattern Recognition* (2022), 108777.
- [11] Geoff French, Timo Aila, Samuli Laine, Michal Mackiewicz, and Graham Finlayson. 2019. Semi-supervised semantic segmentation needs strong, high-dimensional perturbations. *Proc. British Machine Vis. Conf.* (2019).
- [12] Yixiao Ge, Dapeng Chen, and Hongsheng Li. 2020. Mutual mean-teaching: Pseudo label refinery for unsupervised domain adaptation on person re-identification. *Proc. Int. Conf. Learn. Representations* (2020).
- [13] Jean-Bastien Grill, Florian Strub, Florent Altché, Corentin Tallec, Pierre Richemond, Elena Buchatskaya, Carl Doersch, Bernardo Avila Pires, Zhaohan Guo, Mohammad Gheshlaghi Azar, et al. 2020. Bootstrap your own latent—a new approach to self-supervised learning. *Proc. Advances in Neural Inf. Process. Syst.* 33 (2020), 21271–21284.
- [14] Bharath Hariharan, Pablo Arbeláez, Lubomir Bourdev, Subhransu Maji, and Jitendra Malik. 2011. Semantic contours from inverse detectors. In *Proc. IEEE Int. Conf. Comp. Vis.* IEEE, 991–998.
- [15] Kaiming He, Haoqi Fan, Yuxin Wu, Saining Xie, and Ross Girshick. 2020. Momentum contrast for unsupervised visual representation learning. In *Proc. IEEE Conf. Comp. Vis. Patt. Recogn.* 9729–9738.
- [16] Kaiming He, Xiangyu Zhang, Shaoqing Ren, and Jian Sun. 2016. Deep residual learning for image recognition. In *Proc. IEEE Conf. Comp. Vis. Patt. Recogn.* 770–778.
- [17] Ruifei He, Jihan Yang, and Xiaojuan Qi. 2021. Re-distributing Biased Pseudo Labels for Semi-supervised Semantic Segmentation: A Baseline Investigation. In *Proc. IEEE Int. Conf. Comp. Vis.* 6930–6940.
- [18] Hanzhe Hu, Fangyun Wei, Han Hu, Qiwei Ye, Jinshi Cui, and Liwei Wang. 2021. Semi-Supervised Semantic Segmentation via Adaptive Equalization Learning. *Proc. Advances in Neural Inf. Process. Syst.* 34 (2021).
- [19] Wei-Chih Hung, Yi-Hsuan Tsai, Yan-Ting Liou, Yen-Yu Lin, and Ming-Hsuan Yang. 2018. Adversarial learning for semi-supervised semantic segmentation. In *Proc. British Machine Vis. Conf.*
- [20] Zhanghan Ke, Di Qiu, Kaican Li, Qiong Yan, and Rynson WH Lau. 2020. Guided collaborative training for pixel-wise semi-supervised learning. In *Proc. Eur. Conf. Comp. Vis.* Springer, 429–445.
- [21] Alex Krizhevsky, Ilya Sutskever, and Geoffrey E Hinton. 2012. Imagenet classification with deep convolutional neural networks. *Proc. Advances in Neural Inf. Process. Syst.* 25 (2012).
- [22] Samuli Laine and Timo Aila. 2016. Temporal ensembling for semi-supervised learning. *Proc. Int. Conf. Learn. Representations* (2016).
- [23] Tsung-Yi Lin, Michael Maire, Serge Belongie, James Hays, Pietro Perona, Deva Ramanan, Piotr Dollár, and C Lawrence Zitnick. 2014. Microsoft coco: Common objects in context. In *Proc. Eur. Conf. Comp. Vis.* Springer, 740–755.
- [24] Yuyuan Liu, Yu Tian, Yuanhong Chen, Fengbei Liu, Vasileios Belagiannis, and Gustavo Carneiro. 2021. Perturbed and Strict Mean Teachers for Semi-supervised Semantic Segmentation. *arXiv preprint arXiv:2111.12903* (2021).
- [25] Jonathan Long, Evan Shelhamer, and Trevor Darrell. 2015. Fully convolutional networks for semantic segmentation. In *Proc. IEEE Conf. Comp. Vis. Patt. Recogn.* 3431–3440.
- [26] Takeru Miyato, Shin-ichi Maeda, Masanori Koyama, and Shin Ishii. 2018. Virtual adversarial training: a regularization method for supervised and semi-supervised learning. *IEEE Trans. Pattern Anal. Mach. Intell.* 41, 8 (2018), 1979–1993.
- [27] Roozbeh Mottaghi, Xianjie Chen, Xiaobai Liu, Nam-Gyu Cho, Seong-Wan Lee, Sanja Fidler, Raquel Urtasun, and Alan Yuille. 2014. The Role of Context for Object Detection and Semantic Segmentation in the Wild. In *Proc. IEEE Conf. Comp. Vis. Patt. Recogn.*
- [28] Yassine Ouali, Céline Hudelot, and Myriam Tami. 2020. Semi-supervised semantic segmentation with cross-consistency training. In *Proc. IEEE Conf. Comp. Vis. Patt. Recogn.* 12674–12684.
- [29] Kihyuk Sohn, David Berthelot, Nicholas Carlini, Zizhao Zhang, Han Zhang, Colin A Raffel, Ekin Dogus Cubuk, Alexey Kurakin, and Chun-Liang Li. 2020. Fixmatch: Simplifying semi-supervised learning with consistency and confidence. *Proc. Advances in Neural Inf. Process. Syst.* 33 (2020), 596–608.
- [30] Nasim Souly, Concetto Spampinato, and Mubarak Shah. 2017. Semi supervised semantic segmentation using generative adversarial network. In *Proc. IEEE Int. Conf. Comp. Vis.* 5688–5696.
- [31] Antti Tarvainen and Harri Valpola. 2017. Mean teachers are better role models: Weight-averaged consistency targets improve semi-supervised deep learning results. *Proc. Advances in Neural Inf. Process. Syst.* 30 (2017).
- [32] Jingdong Wang, Ke Sun, Tianheng Cheng, Borui Jiang, Chaorui Deng, Yang Zhao, Dong Liu, Yadong Mu, Mingkui Tan, Xinggang Wang, et al. 2020. Deep high-resolution representation learning for visual recognition. *IEEE Trans. Pattern Anal. Mach. Intell.* 43, 10 (2020), 3349–3364.
- [33] Yulin Wang, Gao Huang, Shiji Song, Xuran Pan, Yitong Xia, and Cheng Wu. 2021. Regularizing deep networks with semantic data augmentation. *IEEE Trans. Pattern Anal. Mach. Intell.* (2021). <https://doi.org/10.1109/TPAMI.2021.3052951>
- [34] Yulin Wang, Xuran Pan, Shiji Song, Thang Luong, Gao Huang, and Cheng Wu. 2019. Implicit Semantic Data Augmentation for Deep Networks. In *Proc. Advances in Neural Inf. Process. Syst.* 12635–12644.
- [35] Yuchao Wang, Haochen Wang, Yujun Shen, Jingjing Fei, Wei Li, Guoqiang Jin, Liwei Wu, Rui Zhao, and Xinyi Le. 2022. Semi-Supervised Semantic Segmentation Using Unreliable Pseudo-Labels. *arXiv preprint arXiv:2203.03884* (2022).
- [36] Enze Xie, Wenhai Wang, Zhiding Yu, Anima Anandkumar, Jose M Alvarez, and Ping Luo. 2021. SegFormer: Simple and efficient design for semantic segmentation with transformers. *Proc. Advances in Neural Inf. Process. Syst.* 34 (2021).
- [37] Qizhe Xie, Zihang Dai, Eduard Hovy, Thang Luong, and Quoc Le. 2020. Unsupervised data augmentation for consistency training. *Proc. Advances in Neural Inf. Process. Syst.* 33 (2020), 6256–6268.
- [38] Qizhe Xie, Minh-Thang Luong, Eduard Hovy, and Quoc V Le. 2020. Self-training with noisy student improves imagenet classification. In *Proc. IEEE Conf. Comp. Vis. Patt. Recogn.* 10687–10698.
- [39] Lihe Yang, Wei Zhuo, Lei Qi, Yinghuan Shi, and Yang Gao. 2021. ST++: Make Self-training Work Better for Semi-supervised Semantic Segmentation. *arXiv preprint arXiv:2106.05095* (2021).
- [40] Jianlong Yuan, Zelu Deng, Shu Wang, and Zhenbo Luo. 2020. Multi receptive field network for semantic segmentation. In *Proc. Winter Conf. on Appl. of Comp. Vis.* IEEE, 1883–1892.
- [41] Jianlong Yuan, Yifan Liu, Chunhua Shen, Zhibin Wang, and Hao Li. 2021. A Simple Baseline for Semi-supervised Semantic Segmentation with Strong Data Augmentation. In *Proc. IEEE Int. Conf. Comp. Vis.* 8229–8238.
- [42] Sangdoon Yun, Dongyoon Han, Seong Joon Oh, Sanghyuk Chun, Junsuk Choe, and Youngjoon Yoo. 2019. Cutmix: Regularization strategy to train strong classifiers with localizable features. In *Proc. IEEE Int. Conf. Comp. Vis.* 6023–6032.
- [43] Pan Zhang, Bo Zhang, Ting Zhang, Dong Chen, and Fang Wen. 2021. Robust mutual learning for semi-supervised semantic segmentation. *arXiv preprint arXiv:2106.00609* (2021).
- [44] Wenwei Zhang, Jiangmiao Pang, Kai Chen, and Chen Change Loy. 2021. K-Net: Towards Unified Image Segmentation. In *Proc. Advances in Neural Inf. Process. Syst.*
- [45] Hengshuang Zhao, Jianping Shi, Xiaojuan Qi, Xiaogang Wang, and Jiaya Jia. 2017. Pyramid scene parsing network. In *Proc. IEEE Conf. Comp. Vis. Patt. Recogn.* 2881–2890.
- [46] Yuanyi Zhong, Bodi Yuan, Hong Wu, Zhiqiang Yuan, Jian Peng, and Yu-Xiong Wang. 2021. Pixel Contrastive-Consistent Semi-Supervised Semantic Segmentation. In *Proc. IEEE Int. Conf. Comp. Vis.* 7273–7282.
- [47] Bolei Zhou, Hang Zhao, Xavier Puig, Sanja Fidler, Adela Barriuso, and Antonio Torralba. 2017. Scene parsing through ade20k dataset. In *Proc. IEEE Conf. Comp. Vis. Patt. Recogn.* 633–641.
- [48] Yuliang Zou, Zizhao Zhang, Han Zhang, Chun-Liang Li, Xiao Bian, Jia-Bin Huang, and Tomas Pfister. 2021. PseudoSeg: Designing Pseudo Labels for Semantic Segmentation. *Proc. Int. Conf. Learn. Representations* (2021).